

Article

Nitrogen Removal from the Simulated Wastewater of Ionic Rare Earth Mining Using a Biological Aerated Filter: Influence of Medium and Carbon Source

Silin Chen ^{1,2}, Chengxiu Wu ^{1,2}, Benru Song ^{1,2}, Philip Antwi ^{1,2} , Ming Chen ^{1,2} and Wuhui Luo ^{1,2,3,*}

¹ Jiangxi Key Laboratory of Mining & Metallurgy Environmental Pollution Control, Jiangxi University of Science and Technology, Ganzhou 341000, China; csl1801@163.com (S.C.); 18470720837@163.com (C.W.); songbenru@163.com (B.S.); kobbyjean@yahoo.co.uk (P.A.); cm@jxust.edu.cn (M.C.)

² School of Resources and Environmental Engineering, Jiangxi University of Science and Technology, Ganzhou 341000, China

³ Ganzhou Technology Innovation Center for Mine Ecology Remediation, Ganzhou 341000, China

* Correspondence: luo070221@126.com

Abstract: In engineering application, a two-stage biological aerated filter (BAF) has been deployed to achieve the steady nitrogen removal of the wastewater from the mining area of ionic rare earth with a low carbon to nitrogen (C/N) ratio. However, the cost-efficiency of the medium and carbon source casts a shadow over further development. In this study, the influences of four media (i.e., volcanic, zeolite, quartz, and ceramisite) and three soluble carbon sources (i.e., acetate, glucose, and methanol) on the N removal were systematically compared. Applying volcanic and quartz showed a favorable start-up performance due to the biophilic surface and dense packing, respectively. However, regardless of medium type, with $[\text{NH}_4^+\text{-N}]_0 = 50$ and $[\text{NO}_3^-\text{-N}]_0 = 30$ mg/L, the C/N ratio of 3 was required to meet the discharge standards of $\text{NH}_4^+\text{-N}$, TN, and COD, and acetate was confirmed applicable for all the selected medium-packed BAFs. Introduction of sweet potato residues as the solid carbon source decreased the amount of added acetate by more than 13%. The 16S rRNA high-throughput gene sequencing revealed that *Sphingomonas* and *Nitrospira* were abundant in the aerobic stages of the volcanic and zeolite-packed BAFs, respectively. Such a community integrated with the extensively distributed *Thauera*, *Clostridium_sensu_stricto*, and *Proteiniclasticum* in the anoxic stage accounted for the efficient N removal. Thus, deploying volcanic as the medium and acetate as the soluble carbon source was proposed. These findings will provide valuable references for the selection of medium and carbon source and, consequently, further optimize the operational performance.

Keywords: nitrogen removal; ionic rare earth; BAF; medium; carbon source



Citation: Chen, S.; Wu, C.; Song, B.; Antwi, P.; Chen, M.; Luo, W. Nitrogen Removal from the Simulated Wastewater of Ionic Rare Earth Mining Using a Biological Aerated Filter: Influence of Medium and Carbon Source. *Water* **2022**, *14*, 2246. <https://doi.org/10.3390/w14142246>

Academic Editor: Laura Bulgariu

Received: 19 May 2022

Accepted: 16 July 2022

Published: 17 July 2022

Publisher's Note: MDPI stays neutral with regard to jurisdictional claims in published maps and institutional affiliations.



Copyright: © 2022 by the authors. Licensee MDPI, Basel, Switzerland. This article is an open access article distributed under the terms and conditions of the Creative Commons Attribution (CC BY) license (<https://creativecommons.org/licenses/by/4.0/>).

1. Introduction

The growing demand and inefficient use of nitrogen (N) in agriculture and industry is transforming the global N cycle and causing a cascade of environment problems. Decreasing the discharge of N-bearing wastes into the environment to minimize the negative consequences is of significance [1]. Ammonia gas (NH_3), as the reduced form of N, produced from the Haber-Bosch process is a raw material that is extensively used in manufacturing various products, such as ammonium salts (NH_4^+), plastics, etc. NH_4^+ is the conjugated acid of NH_3 and has attracted wide attention due to its high solubility and the high impacts on the environmental system. Recovery of $\text{NH}_4^+\text{-N}$ from aqueous solution is one of the key steps to alleviate the influence of anthropogenic activities on the global N cycle. Compared with air stripping [2], membrane separation [3], and adsorption [4], biological treatment is a relatively low-cost technique that can efficiently transform $\text{NH}_4^+\text{-N}$ without secondary pollution and is still the recommended method in most cases [5,6].

A biological aerated filter (BAF) is an effective and flexible bioreactor that contains medium serving as the habitat for the microorganisms to assimilate N, phosphorus, and

organic matters in the wastewater [7]. A BAF provides many advantages, including a smaller footprint, less sludge production, and higher biomass [8–10], but there are also some deficiencies when BAF is applied for NH_4^+ -N removal, such as low resistance of the influent with the high concentrations of suspended solids (SS) and organics. A high SS concentration requires frequent backwashing, and the concentrated organics facilitate the growth of heterotrophic bacteria that will restrain the activity and population of the autotrophic nitrifier due to the consumption of dissolved oxygen (DO) [11]. However, for the single-stage BAF, a certain concentration of organics is required in the influent as the electron donor for denitrification [12], suggesting that the conventional BAF is merely suitable for the treatment of some particular wastewater. In fact, BAF is widely used for simultaneous removal of N and organics. To achieve a favorable performance, the BAF was normally operated stringently or integrated with other processes. Yang et al. [13] deployed the strengthened circulation anaerobic process to combine with the BAF, achieving the efficient removal of N in municipal wastewater. A two-stage BAF was developed by An et al. [14] in which the second stage operated with the smaller aeration rate (80 L/h) showing the higher removal rate of N. Landfill leachate with high concentrations of NH_4^+ -N and organics was coped with a zeolite BAF prefixed with the denitrification stage [15], showing a removal efficiency of NH_4^+ -N and total nitrogen (TN) of 93.5% and 74.7%, respectively. For the treatment of a specific wastewater, the water characteristics-oriented modification for the conventional BAF is needed.

Due to the usage of $(\text{NH}_4)_2\text{SO}_4$ as the leaching agent, the tailing wastewater from the mine area of ionic rare earth that is mainly distributed in the southern provinces of China contains high concentrations of NH_4^+ -N and nitrate nitrogen (NO_3^- -N) [16]. In addition, the wastewater contains low total SS (Table 1) and is well-matched for the influent requirements of BAF, suggesting the potential application of BAF in the treatment of such a wastewater. However, this has not yet been reported. Moreover, because the wastewater has the low organic concentration and TN is involved in the discharge standards, the single-stage BAF is incapable of meeting the requirement. Thus, the conventional BAF suffixed with a denitrification stage (Figure 1) was proposed and applied in the engineering. For further development, the cost-efficiency of the medium and carbon source is urgent to improve.

The packing medium and water characteristics are important factors influencing the microbial community in the BAF and, consequently, determining the treatment efficiency for pollutants. Ji et al. [11] applied clinoptilolite and metallic iron-supplemented coal ash bioceramsite to form a multimedia BAF, where increasing the content of metallic iron decreased the percentage of anaerobic ammonia-oxidizing bacteria but increased the N removal efficiency. In fact, the packing medium also has significant influences on the biofilm formation and hydraulic characteristics and normally should be chemically stable and attrition-resistant [17]. Thus, a variety of inorganic materials, including zeolite, grain-slag, ceramsite, sand, carbonate medium, etc., were used as biofilm carriers in BAFs [11,18–20]. In terms of NH_4^+ -N removal efficiency, Qiu et al. [20] proposed that zeolite was a more suitable medium for nitrification than carbonate and ceramsite due to the high ion exchange capacity, and Feng et al. [19] found that the calcium carbonate-bearing grain slag was better than haydite due to the pH buffering effect. For a single- or multistage BAF operated at different conditions, the most suitable medium may be different. In addition, due to the low carbon (C)/N ratio of some raw influents, the additional carbon is required to ensure the denitrification process, typically such as methanol, ethanol, glucose, acetic acid, and sodium acetate [6,21–23]. These water-soluble but costly carbon sources are widely used due to the easy dissolution, high bioavailability, and fast reaction speed. Aiming to search for alternatives, in recent years researchers are struggling to search for nontoxic and cheap solid carbon sources that are abundant in cellulose and sustained in carbon release, such as plant straw [24,25], wood-chips [26], and bark [27]. However, these natural cellulose-rich sources normally possess stable structure, resulting in the insufficient release of carbon and changing the microbial community and, consequently, leading to poor denitrification performance [28]. Jiang et al. [29] compared the composition of the microbial communities

using polycaprolactone and acetate as the carbon sources, where a larger quantity of *Proteobacteria* but poorer denitrification performance was observed for the former case due to the inappropriate ratio of micro-organisms accounting for decreasing NO_3^- -N and chemical oxygen demand (COD). Selecting a solid carbon source that can continuously provide enough bioavailable carbon is still challenging.

Table 1. Characteristics of the tailing wastewater from the mining area of ionic rare earth.

Parameter	COD _{Cr} (mg/L)	NH ₄ ⁺ -N (mg/L)	TN (mg/L)	TP (mg/L)	pH	TSS
Range	10~30	40~70	60~130	0.01~0.5	4.0~6.0	10~20
Standards *	70	15	30	1	6.0~9.0	50

Note: * Emission Standard of Pollutants for Rare Earths Industry (GB 26451-2011).

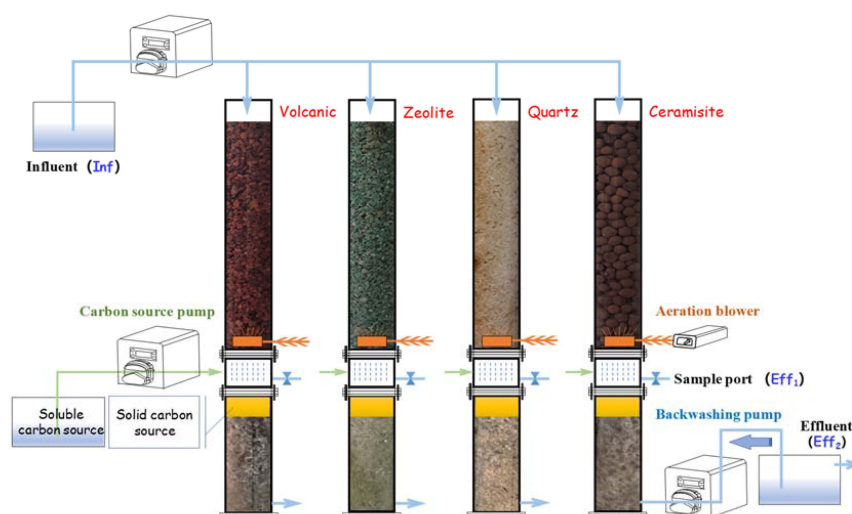


Figure 1. Schematic diagram of the constructed BAF.

Thus, to this end, the integrated BAF (Figure 1) is designed for the removal of N in the simulated tailing wastewater, and the specific aims of this work included: (1) to systematically investigate the influences of four filter media—volcanic, zeolite, quartz, and ceramisite—on the biofilm culturing and N removal characteristics, which have not been compared under the same operational condition in such an integrated BAF; (2) to optimize the operation status via comparing the routinely used methanol, glucose, and acetate as carbon sources, considering that the denitrification performance with a specific carbon source seems reactor-dependent [21,22,30]; (3) to test the applicability of sweet potato residues (SPR) as a solid carbon source considering the massive destarching process of sweet potato and the inadequate usage of the residues in China [31]; the rice husk was also selected as another solid carbon source for comparison. Lastly, (4) the microbial community was identified using the 16S rRNA high-throughput gene sequencing technology to determine the predominant micro-organisms responsible for N removal in the process.

2. Materials and Methods

2.1. Materials and Reagents

According to the compositions of the tailing wastewater (Table 1), the synthetic influent was prepared through dissolving $(\text{NH}_4)_2\text{SO}_4$ (~50 mg/L NH_4^+ -N) and NaNO_3 (~30 mg/L NO_3^- -N) salts in tap water. A small amount of phosphate was added to ensure the metabolism of the micro-organisms, and sodium bicarbonate (NaHCO_3 , ~600 mg/L) was deployed to achieve the appropriate pH and provide inorganic carbon for the nitrifiers [19].

2.2. Reactor Description, Start-Up and Operation

As shown in Figure 1, the reactor with an inner diameter of 70 mm and a total volume of 4.5 L was constructed with acrylic, and each reactor consists of two main stages, i.e., aerobic zone ($H_1 = 63 \pm 2$ cm) and anoxic zone ($H_2 = 35$ cm). The air diffuser was installed at the bottom of the aerobic stage to introduce O_2 for the nitrification. The synthetic wastewater was fed to the reactor with down-flow mode, and the additional soluble carbon was imported before the anoxic stage by a peristaltic pump (BT100L, Leadfluid, Baoding, China). At the outlet, another peristaltic pump was set to control the hydraulic loading rate (HLR) and conduct the water backwash, where air scour was not adopted to maintain the anaerobic condition. Notably, four parallel reactors were operated periodically (3 days), consisting of (1) shutting off the influent and carbon source (~5 h) to expose the aerobic zone to air and restrain the biomass production on the first day, (2) conducting water backwash (~100 mL/min) for several minutes to reimmerge the aerobic zone, and (3) keeping the immersed status running until the end of the period. With such a procedure, reactors were steady operated without visible blockage. Each operational condition was maintained for at least 4 periods (>12 days) to stabilize the system before switching to other conditions.

2.3. Analytic Methods

The effluent samples were filtered through 0.45- μ m cellulose acetate filter and collected in airtight bottles in a refrigerator before the batch analysis. The concentrations of NH_4^+ -N, NO_3^- -N, nitrite (NO_2^- -N), and COD were determined according to the standard methods. The DO and pH were measured using a portable oxygen meter (JPB-607A, LEICI, Shanghai, China) and a proton meter (PXSJ-266, LEICI, Shanghai, China), respectively.

2.4. Characterization of Filter Media

The physical characteristics of the original filter media are shown in Table 2, where N_2 adsorption-desorption isotherms (ASAP 2020HD88, Micromeritics, Atlanta, GA, USA) and mercury intrusion porosimetry (AutoPore IV 9500, Micromeritics, Atlanta, GA, USA) were deployed to obtain the specific surface area considering the different properties of the media. Additionally, a scanning electron microscope (PQ9000, Analytik Jena, Jena, Germany) was used to observe the changes of media surfaces after microbial interactions. Notably, all filter media were not ground and directly used for the characterization.

Table 2. Physical properties of the filter media.

Parameter/Media	Volcanic	Zeolite	Quartz	Ceramisite	
Size (mm)	3~6	3~6	2~4	8~10	
Surface area (m^2/g)	Original	17.5 ^a	16.4 ^b	0.3 ^b	13.3 ^a
	Aerobic stage	10.8	14.7	n.a.	16.1
	Anoxic stage	5.8	15.4	n.a.	19.8
Porosity (%)	25.5 ^a	2.3 ^b	0.1 ^b	76.9 ^a	
Density (g/cm^3)	2.15 ^a	2.17 ^c	2.61 ^c	0.49 ^a	

Notes: ^a Based on mercury porosimetry data analyzed by the Washburn equation. ^b Based on N_2 adsorption-desorption isotherms analyzed by the Brunauer-Emmett-Teller equation. ^c Measured according to the Filter Material for Water Treatment (CJ/T43-2005).

2.5. Analysis of Microbial Community

At each stage, the sludge adhering to the filter media was rinsed away and collected for further analysis. Assisted with the E.Z.N.A™ Mag-Bind DNA Kit (OMEGA, Norwalk, CT, USA), the total genomic deoxyribonucleic acid (DNA) of each sample was extracted, which was followed by the DNA quality inspection via agarose gel electrophoresis. After being quantified by Qubit 3.0 DNA Detection Kit (Life Technologies, ThermoFisher, Waltham, MA, USA), the V3~V4 regions of 16S rRNA genes were amplified with primers (Nobar_341F: 5'-CCT ACG GGN GGC WGC AG-3' and Nobar_805R: 5'-GAC TAC HVG GGT ATC TAA

TCC-3') for two rounds to minimize PCR biases. The qualified DNA was finally sequenced with an Illumina MiSeq platform (Vazyme Biotech Co., Ltd., Piscataway, NJ, USA), and the sequences were classified into operational taxonomic units (OTU) and assigned to the corresponding taxonomies when the similarity and coverage are over 97%.

3. Results and Discussions

3.1. Physical Characteristics of Filter Media

As shown in Figure 2, volcanic, zeolite, and ceramisite possess the rough surface that will be conducive for micro-organism adhesion [32], while it is hard to find the biofilm on the filters in the aerobic stage, which can be attributed to intensive attrition with the air bubbles and the adjacent particles. However, a thick film was formed on the volcanic, likely due to the aggregation of the nanosized volcanic particles with the extracellular polymeric substance. Compared with the filter media in the aerobic stage, those in the anoxic stage showed more remarkable changes with visible trails of bacterial interactions, where the flake-like, wirelike, and/or netlike substances were observed on the surfaces. This suggests that the relatively weak turbulence is beneficial for the formation of biofilm. In addition, due to the interactions with the micro-organism, the surface areas of the filter media were also changed differently (Table 2). For the volcanic in the anoxic stage, the surface area was decreased significantly because of the intensive coverage of the surface (Figure 2), while only negligible changes were observed for zeolite and quartz. Generally, the surface area is mainly derived from the nanopores of the material. Zeolite possesses nanopores that are inaccessible for bacteria, resulting in the slight change after the interactions. Interestingly, far different from the other media, the surface area of ceramisite was increased regardless of the stages. As shown in the SEM images, there are tons of macropores for ceramisite (Figure 2), which is consistent with the high porosity (Table 2). However, Bao et al. [33] proposed that commercially available ceramisite has a less open macropores structure with respect to the autoclaved aerated concrete particles, which resulted in the smaller amount of micro-organisms immobilized. Although it is hard to find the loaded bacteria on the external surface, the metabolites and/or bacteria themselves might penetrate into the macropores and regenerate new nanopores that greatly contribute to the rise of surface area.

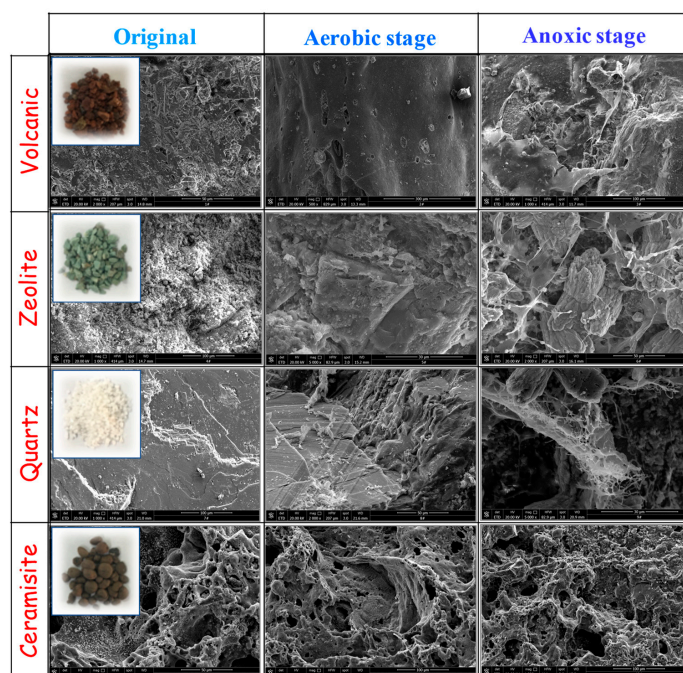


Figure 2. SEM images of filter media in different stages.

3.2. Start-Up Performance of Reactors

For the start-up period, the same amount of seed activated sludge was introduced into four reactors, and only ~50 mg/L of $\text{NH}_4^+\text{-N}$ was involved in the influent to lower the N burden. At the corresponding inlets, bicarbonate and acetate were pumped as the carbon sources for the autotrophic nitrifiers and heterotrophic denitrifiers, respectively. To ensure enough electron donors for the denitrification process, the C/N ratio was set at 5. As shown in Figure 3, the concentration of $\text{NO}_3^-\text{-N}_{\text{Eff}1}$ shows the gradient increase until close to that of imported $\text{NH}_4^+\text{-N}$, indicating the gradual accumulation and adaption of the nitrifiers and the eventual completion of the nitrification process. Considering that the fresh media packed in the reactors may adsorb $\text{NH}_4^+\text{-N}$ through the ion exchange or surface adsorption [34], the static adsorption test was performed and the results are shown in Figure 4a. Zeolite and volcanic can partially capture $\text{NH}_4^+\text{-N}$ from the aqueous solution, while quartz and ceramisite are incapable, the same as the reported [32]. This may account for the absence of $\text{NH}_4^+\text{-N}_{\text{Eff}1}$ and $\text{NH}_4^+\text{-N}_{\text{Eff}2}$ at the early stage of the start-up in these two reactors. In addition, although zeolite is a cationic clay mineral with a negatively charged framework, a remarkable and rapid uptake for $\text{NO}_3^-\text{-N}$ (~0.15 mg-N/g) was observed (Figure 4b). However, the concentration of $\text{NO}_3^-\text{-N}_{\text{Eff}2}$ in the zeolite reactor was higher than that in the other reactors, implying that the removal of $\text{NO}_3^-\text{-N}$ was mainly ascribed to the microbial denitrification rather than adsorption.

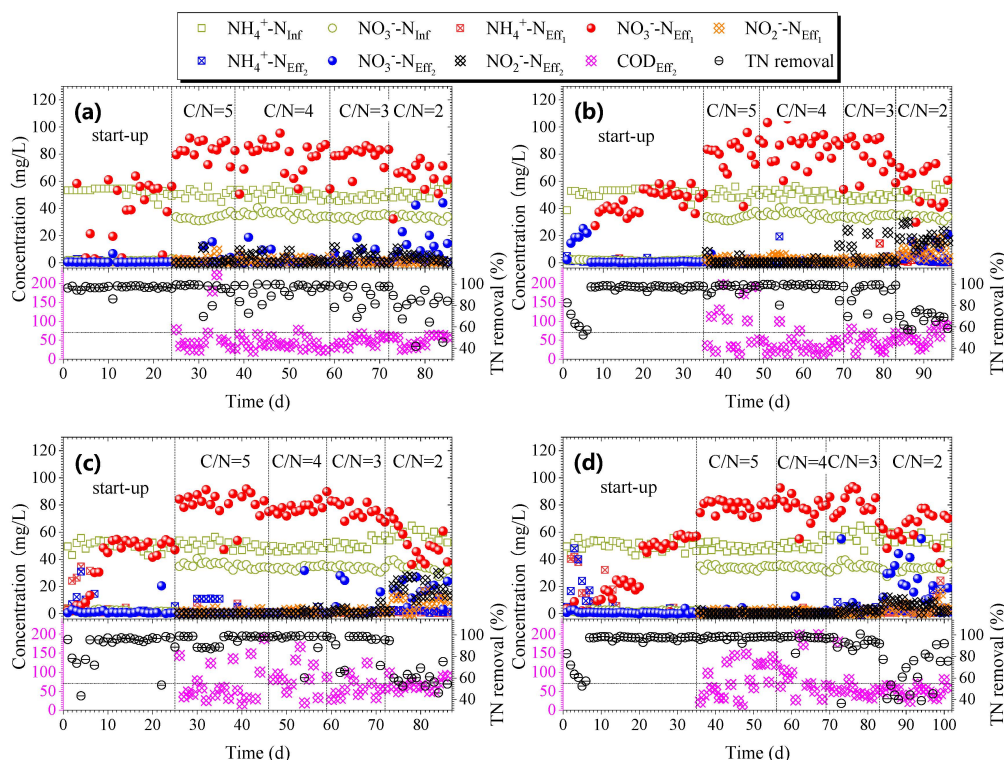


Figure 3. Start-up performance and C/N ratio influence on N removal in (a) volcanic-, (b) zeolite-, (c) quartz-, and (d) ceramisite-packed reactors.

In terms of the time-efficiency, volcanic and quartz are suitable to achieve a rapid start-up, where only ~10 days is required to achieve the completed nitrification, far shorter than the CANON process (~26 days) [35]. This is because of the rougher external surface of volcanic and the smaller size of quartz with respect to the other two media. Although it has been proposed that the porosity and pore size rather than the surface property of supports played the major role in the biofilm formation [36], the coarse surface will contribute to the attachment of micro-organisms, and the smaller space among particles derived from the denser packing is favorable for the bacteria to accumulate and survive. Notably, the TN

removal was over than 90% within 10 days in four reactors. However, in order to achieve the steady nitrification and denitrification performance, different days are assigned to the start-up period.

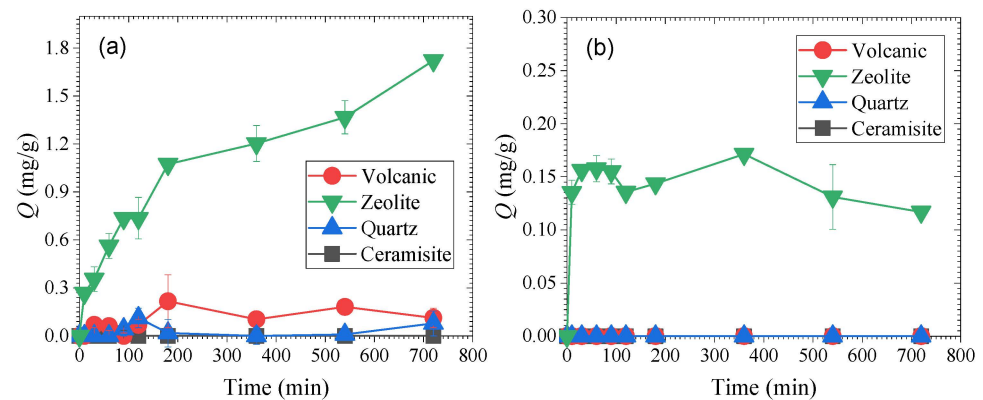


Figure 4. Adsorption kinetics of the applied filter media for (a) $\text{NH}_4^+\text{-N}$ and (b) $\text{NO}_3^-\text{-N}$ ($[\text{NH}_4^+\text{-N}]_0 = [\text{NO}_3^-\text{-N}]_0 = 50 \text{ mg/L}$, $V = 600 \text{ mL}$, $m = 10 \text{ g}$, $T = 25 \text{ }^\circ\text{C}$, 200 rpm).

3.3. Influence of C/N Ratio on the Performance of N Removal

On the heels of the start-up, the C/N ratio was decreased gradually from 5 to 2 to save energy. Meanwhile, $\sim 30 \text{ mg/L}$ of $\text{NO}_3^-\text{-N}$ was added in the feedstock to simulate the tailing wastewater from the mining area of ionic rare earth (Table 1). Considering that a relatively high C/N ratio may result in COD in effluent over the borderline concentration (70 mg/g), the COD of the entire process was also determined at the same time. Notably, because the simulated wastewater was prepared using tap water where the COD was determined to be around 1.0 mg/L , such a low concentration of the indigenous organics would pose negligible influence. Thus, the influent COD derived from the external added carbon at the beginning of the denitrification stage was directly calculated based on the applied C/N ratio. For instance, when a C/N ratio of 3 was deployed, the added carbon should ensure a COD of 240 mg/L assuming $\text{NH}_4^+\text{-N}$ was completely oxidized in the nitrification stage. As shown in Figure 3, except for a few days, the concentrations of N in the terminal effluent (Eff2) are low enough to meet the Emission Standard of Pollutants for Rare Earths Industry (GB 26451-2011, Table 1) until the C/N ratio of 2. However, in the volcanic reactor, the TN removal is still higher than 80% for most cases, even when offered a low C/N ratio, and the injected carbon was efficiently consumed judging from the concentration of COD_{Eff2} . This suggests that volcanic is a more suitable filter medium, which is consistent with the result proposed by Dong et al. [18]. Interestingly, accompanied with the decrease of C/N ratio from 3 to 2, the visible drop of $\text{NO}_3^-\text{-N}_{\text{Eff1}}$ concentration and the presence of $\text{NH}_4^+\text{-N}_{\text{Eff1}}$ and/or $\text{NO}_2^-\text{-N}_{\text{Eff1}}$ were observed, suggesting that the short-cut nitrification and denitrification might be occurring in the aerobic zone. At the C/N ratio of 2, the small gap of $\text{NO}_3^-\text{-N}$ concentration between Eff1 and Eff2 solidly confirmed the insufficient denitrification. Consequently, the average removal efficiency of N in the volcanic-, zeolite-, quartz-, and ceramisite-packed reactors were around 75%, 55%, 62%, and 64%, respectively. Thus, to ensure a satisfying performance, the C/N ratio of 3 was selected for the following tests.

3.4. Influence of Hydraulic Loading Rate on the Performance of N Removal

Increasing the flow rate, namely shortening the hydraulic retention time (HRT), will decrease the contact time and mass transfer process between micro-organism and substrate, resulting in insufficient N removal. As shown in Figure 5, duplicating the flow rate from 2 to 4 mL/min , corresponding to the increase of hydraulic loading rate (HLR) from 0.7 to $1.4 \text{ m}^3/(\text{m}^2 \cdot \text{d})$, led to the unfavorable performance as supported by the high concentrations of $\text{NO}_3^-\text{-N}$ and COD in Eff2. However, the N concentrations in the Eff1 seem negligibly affected by the increased flow rate, showing the strong resistance of the aerobic stage [18].

This implies that lengthening the anoxic stage is necessary to optimize the operation performance in the future. Among the four reactors, the ceramisite-packed performed best, evidenced by the relatively steady and low N and COD concentrations. In the same reactor, because of the different porosity and shape of the filter, the effective volume should be different. The HRT estimated are 10.9, 8.5, 7.5, and 8.75 h for the volcanic-, zeolite-, quartz-, and ceramisite-packed BAFs when the flow rate of 2 mL/min was applied, respectively. These are close to the operational condition that was applied to deal with the landfill leachate using a BAF [37]. Ceramisite, as a spherical particle with high porosity (Table 2), provides the greater space for the wastewater with moderate HRT, ensuring the interactions of bacteria with the involved nutrition.

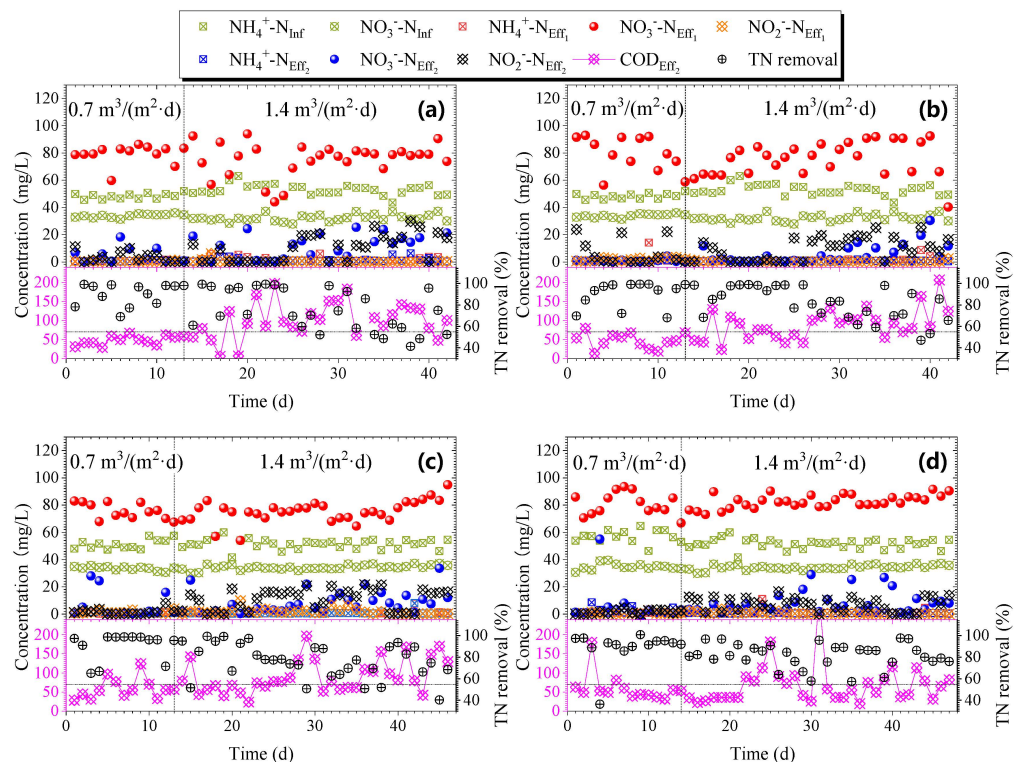


Figure 5. Influence of hydraulic loading rate on N removal in the (a) volcanic-, (b) zeolite-, (c) quartz-, and (d) ceramisite-packed reactors.

3.5. Influence of Carbon Source on the Performance of N Removal

3.5.1. Water-Soluble Carbon Source

As shown in Figure 6, three typical soluble carbon sources (acetate, glucose, and methanol) were applied, and the N removal performance seems carbon- and/or filter medium-dependent. With the C/N ratio of 3, in most cases the COD_{Eff2} of all reactors with different soluble carbon sources were lower than the emission standard, indicating that three carbon sources are bioabsorbable. However, the N removal in different reactors varied significantly. Although the soluble carbon was introduced merely for the anoxic stage through the downward flow (Figure 1), some of them may diffuse to the aerobic stage. With the concentrations of DO_{Eff1} within 3–5 mg/L, other N removal processes, such as the short-cut nitrification and denitrification and CANON, seem less likely to occur in the nitrification stage [38]. However, considering the heterogeneous distribution of O_2 derived from the medium packing and biofilm growth in the bulk system, there may be some interior spaces possessing the low DO concentrations, and in which these processes might happen at the appropriate organic concentrations. This is also supported by the low concentrations of $NO_2^- - N_{Eff1}$. As a result, the concentration of $NO_3^- - N_{Eff1}$ changed significantly with the different carbon sources. For all filter media, applying acetate as the carbon source,

the nitrification proceeded well as supported by the high concentration of $\text{NO}_3^- - \text{N}_{\text{Eff}1}$; however, when glucose and methanol were used, the nitrification was negatively influenced. Additionally, combined with the $\text{COD}_{\text{Eff}2}$ values, the small concentration gap between $\text{NO}_3^- - \text{N}_{\text{Eff}1}$ and $\text{NO}_3^- - \text{N}_{\text{Eff}2}$ in the quartz and ceramisite reactors (Figure 6c,d) suggests that these two carbon sources are mainly used for the biomass production rather than the electron donor for denitrification. Compared with acetate, glucose requires enzymatic conversion before incorporating into the metabolism of most denitrifying bacteria [39], while methanol, as a liquid form, is hard to transport and store and will inactivate the microorganisms with the excess concentrations. Thus, acetate is proposed as the soluble carbon source for the designed reactors. Fu et al. [40] also concluded that sodium acetate would be the first choice through reviewing the effects of external carbon sources on denitrification.

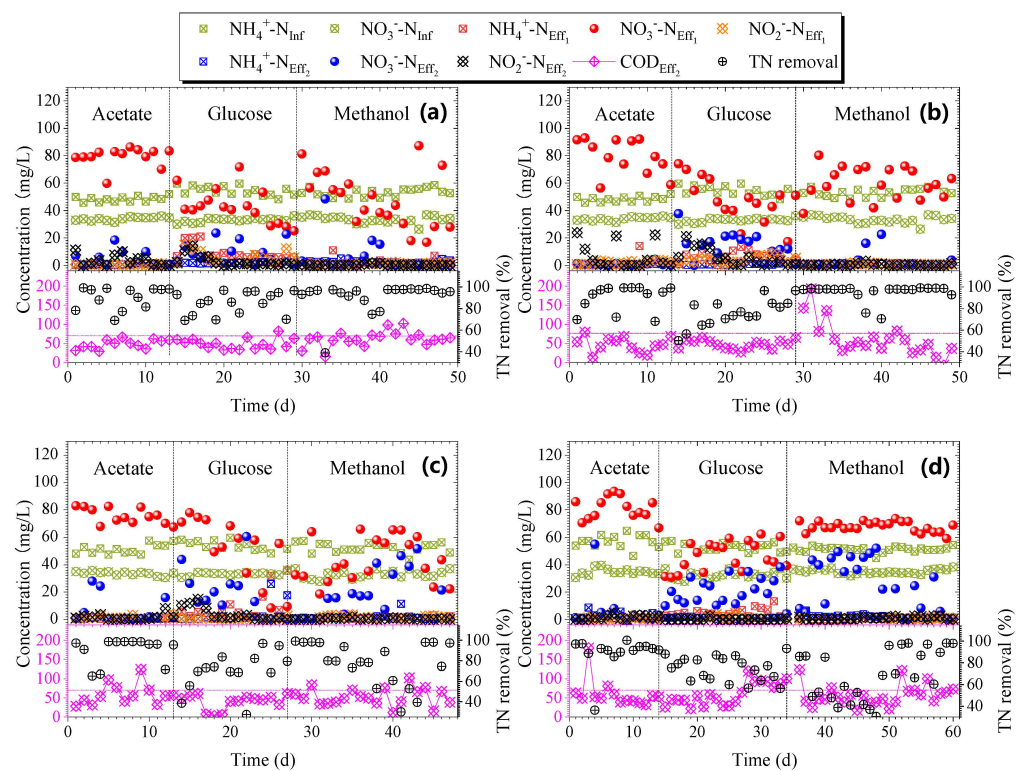


Figure 6. Comparison of the N removal performance using acetate, glucose, and methanol as liquid carbon source in the (a) volcanic-, (b) zeolite-, (c) quartz-, and (d) ceramisite-packed reactors.

3.5.2. Solid Carbon Source

As shown in Figure 1, at the top of the anoxic stage, at around 5 cm depth, the filter media was replaced by solid carbon. Based on the previous results, the volcanic-packed reactor was selected to investigate the performance of sweet potato residue (SPR) in carbon release. As shown in Figure 7, in the first 12 days, with the soluble-C/N ratio of 3, the concentration of $\text{COD}_{\text{Eff}2}$ was significantly higher than the discharge standard and that without SPR addition (Figure 6a), which should be ascribed to the release of carbonaceous matter from the SPR. Reducing gradually the amount of the introduced soluble carbon, i.e., decreasing the C/N ratio from 3 to 2.6, still ensures the low N concentrations in Eff2 on the premise that the $\text{COD}_{\text{Eff}2}$ concentration is discharge-qualified. This suggests that deploying SPR as the solid carbon source to partially provide carbonaceous matter for the denitrifying bacteria is applicable and will save more than 13% of the costs of using the soluble carbon. Considering that the release of carbonaceous matter from the SPR will be decreased with time [41,42] and the performance of TN removal with a C/N of 2.6 seems unsteady, the tests with the lower C/N ratios were not carried out. Notably, because ~14% (v/v) volcanic was replaced by the powdery SPR, the backwash became insufficient after

running for 1 month. Immobilizing these fine and flowable solid carbon particle is essential from a long-term perspective. For a specific solid carbon source, it is hard to have both efficient carbon release and no blockage, which is still the technical bottleneck to achieve engineering applications [40]. Rice husk, as a centimeter-sized agricultural waste, was also used to test the capability of releasing bioavailable carbon in the quartz- and ceramisite-packed reactors. Although the blocking was visible, the release of carbon was negligible or unstable (Figure S1). However, Luo et al. [43] found that adding rice husk into a long-term flooded constructed wetland could be conducive to completing the nitrification process. Notably, the influence of introducing SPR and rice husk on N removal was conducted in winter, when the temperatures of influent and effluent are around 16 °C. It is inevitable to suffer such a harsh condition for the bio-treatment of the tailing wastewater from the ionic rare earth mining area. The slow release of carbon from the rice husk [44] and low activity of microbes at low temperatures may account for the unfavorable results with respect to previous reports [42].

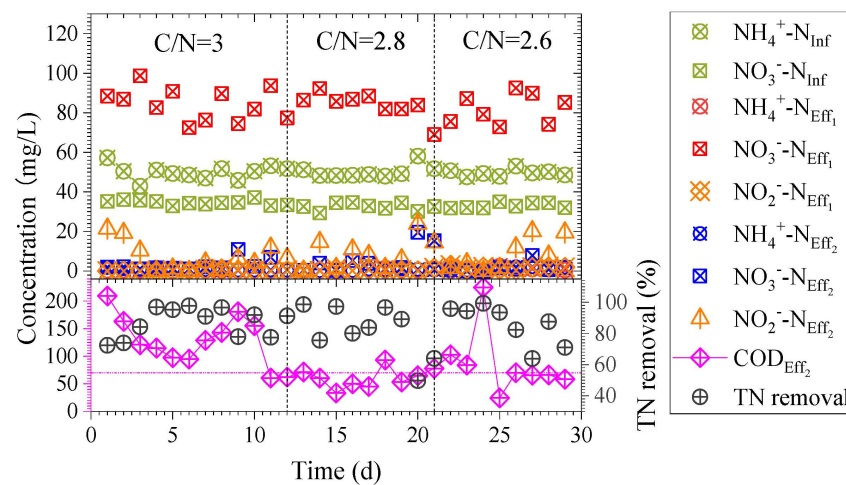


Figure 7. Influence of the sweet potato residue on the N removal performance in the volcanic-packed reactor.

3.6. Bacterial Community Analysis

3.6.1. Diversity of Bacterial Community

In total, there were 20 samples collected from different experimental conditions (Table 3) used for the high-throughput sequencing analysis. The coverage values of more than 0.99 for all samples indicate that the given data can cover most bacterial communities. For the aerobic stage, the total number of OTUs varied significantly with the medium type, where the greatest OTUs for CN suggested the good adaptation of some aerophile bacterial groups to the conditions provided by ceramisite. However, for the anoxic stage, the number of OTUs changed slightly regardless of the medium and soluble carbon species. Notably, increasing the hydraulic loading rate (HLR) remarkably decreased the bacterial richness in the quartz- or ceramisite-packed reactor. The mentioned variations are also well-revealed by the Chao and Ace indices.

To further characterize the abundance and evenness of micro-organisms present in the reactors, Simpson and Shannon indices were introduced for comparison (Figure 8). In general, the Shannon indices of the samples collected from the anoxic stage were greater than those from the aerobic stage, suggesting the expansion of microbial diversity when organic carbon was deployed. However, compared with glucose and methanol, applying acetate as the feeding carbon lowered the bacterial diversity as supported by the smaller Shannon indices. This is attributed to the phase-out of other acetate-specific bacteria resulting from the flourishing of the denitrifying bacteria, which is in accordance with Jiang et al. [45] who found that the highest total relative abundance of denitrifying bacteria in

the denitrification biofilters fed with acetate was observed with respect to that with glucose or methanol.

Table 3. Samples used for high-throughput sequencing analysis.

Experimental Conditions				Analysis						
Sample	Medium	Carbon	Stage	HLR	OTUs	Chao	Ace	Simpson	Shannon	Coverage
VN	Volcanic	/	Nitrification	0.7	737	934.5	920.4	0.833	2.86	0.996
ZN	Zeolite	/			468	587.0	593.2	0.789	2.70	0.996
QN	Quartz	/			992	1115.0	1067.0	0.969	4.29	0.998
CN	Ceramisite	/			1027	1146.1	1120.8	0.948	3.98	0.997
VAD2	Volcanic	Acetate		1.4	786	955.5	957.2	0.955	4.26	0.995
ZAD2	Zeolite				625	808.7	794.5	0.948	4.04	0.993
QAD2	Quartz				364	596.6	582.2	0.929	3.91	0.997
CAD2	Ceramisite				303	445.7	485.6	0.882	3.56	0.997
VAD	Volcanic	Acetate	Denitrification		660	891.0	875.2	0.925	3.44	0.996
ZAD	Zeolite				730	953.3	960.3	0.914	3.31	0.995
QAD	Quartz				717	961.0	932.8	0.942	3.70	0.991
CAD	Ceramisite				737	948.0	973.1	0.940	3.69	0.995
VGD	Volcanic	Glucose		0.7	813	1027.0	1031.5	0.967	4.34	0.993
ZGD	Zeolite				742	1018.3	934.8	0.972	4.39	0.994
QGD	Quartz				656	878.0	878.6	0.943	4.00	0.994
CGD	Ceramisite				784	974.2	935.7	0.964	4.21	0.994
VMD	Volcanic	Methanol			846	1037.2	1048.1	0.969	4.42	0.994
ZMD	Zeolite				734	917.1	917.6	0.971	4.40	0.994
QMD	Quartz				735	943.3	936.2	0.958	4.05	0.997
CMD	Ceramisite				564	751.8	740.4	0.906	3.62	0.991

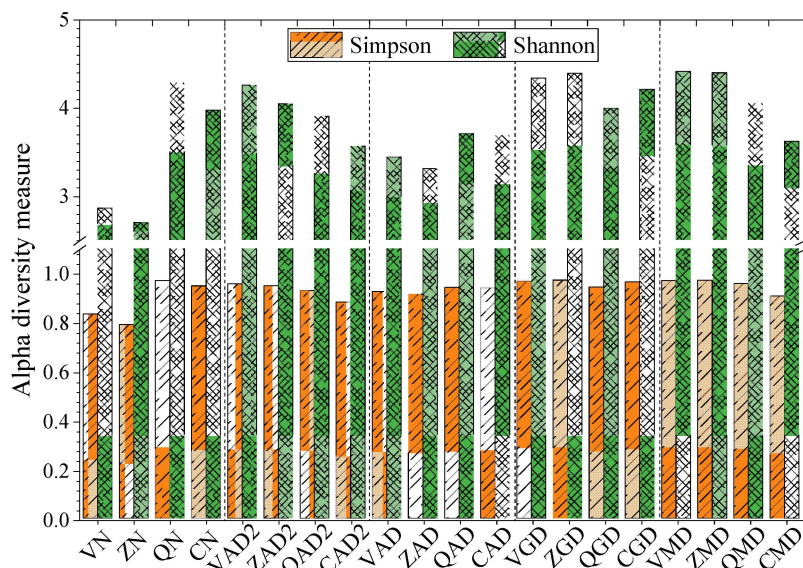


Figure 8. α -diversity analysis using the Simpson and Shannon indices.

The β -diversity results (Figure 9) indicate that the oxygen concentration and soluble carbon type are the key factors significantly impacting the Bray-Curtis distance. Oxygen affected the community the most, which was followed by the species of the soluble carbon. Acetate might stimulate the reproduction of some denitrifying bacteria, accounting for the significant difference in the bacterial community when using acetate and when using the other two as the carbon sources. Lastly, the community was also partially influenced by the hydraulic loading rate because some micro-organisms might be washed off with a high flow rate, showing the structural instability as supported by the divergent data.

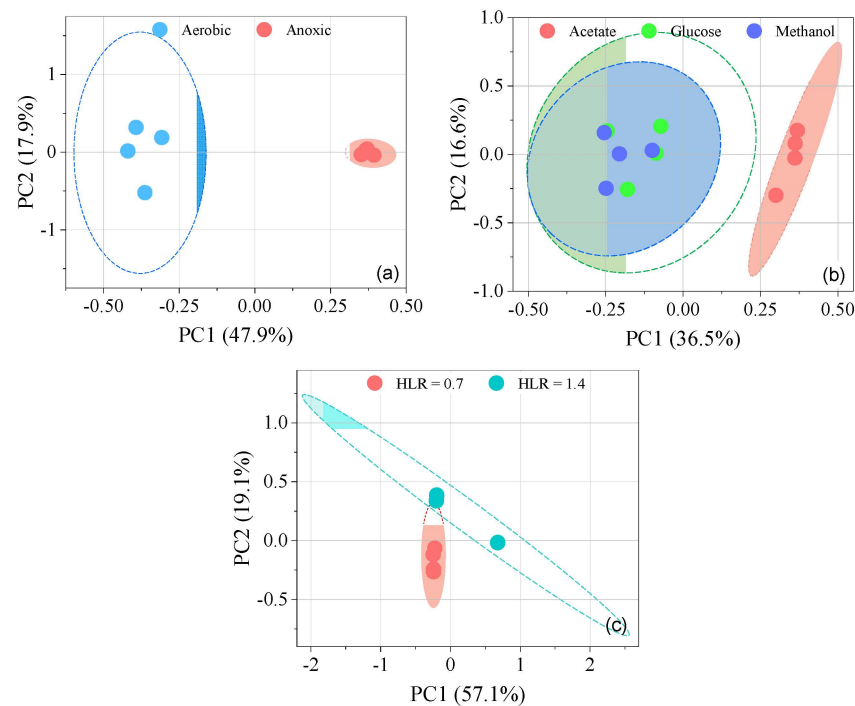


Figure 9. β -diversity analysis of samples in terms of (a) oxygen concentration, (b) soluble carbon species, and (c) hydraulic loading rate.

3.6.2. Composition of Bacterial Community

As shown in Figure 10, the bacterial sequences are classified at phylum and family levels to identify the composition of the bacterial community. At the phylum level (Figure 10a), *Proteobacteria*, as one of the dominant players for N removal and COD degradation [46], was most extensively detected for the majority of reactors. Based on the sequences obtained from the samples of the aerobic stage (VD, ZD, QD, and CD), the relative abundance of *Proteobacteria* (85.3%) is significantly higher in the reactor packed with volcanic with respect to other media. In contrast, the most pronounced phylum affiliated to ZN was *Nitrospirae* (43.7%) which accounts for the nitrite oxidation, and the relative abundances of *Nitrospirae*, *Planctomycetes*, *Firmicutes*, *Acidobacteria*, and *Actinobacteria* are similar for the quartz- and ceramisite-packed reactors. Interestingly, the oligotrophic *Acidobacteria* that widely exists in soil was detected in a large quantity in the QN system. In general, the abundance of *Acidobacteria* is negatively correlated with the system pH [47]; however, the pH of Eff1 (>8.0) from the quartz-packed BAF is higher than that from other systems, suggesting that the abundance of *Acidobacteria* might be influenced by other operational conditions. *Bacteroidetes* mainly presents in anoxic conditions to participate in the denitrification process [46] and is visibly identified in VN, ZN, and QN, likely due to the diffusion of the introduced soluble carbon and the heterogeneous distribution of O_2 in the aerobic zone. Interestingly, over 95% of the obtained sequences from the samples (VAD, ZAD, QAD, and CAD) belonged to *Proteobacteria*, *Bacteroidetes*, *Firmicutes*, and *Actinobacteria*, indicating a relatively simple ecosystem. Thus, the favorable performance of N removal in these four reactors (Figure 6) implies a fine cooperation. *Firmicutes* seems acetatephilic as supported by its prevalence when acetate is applied as the carbon source, which is likely responsible for the relatively steady N removal and COD degradation.

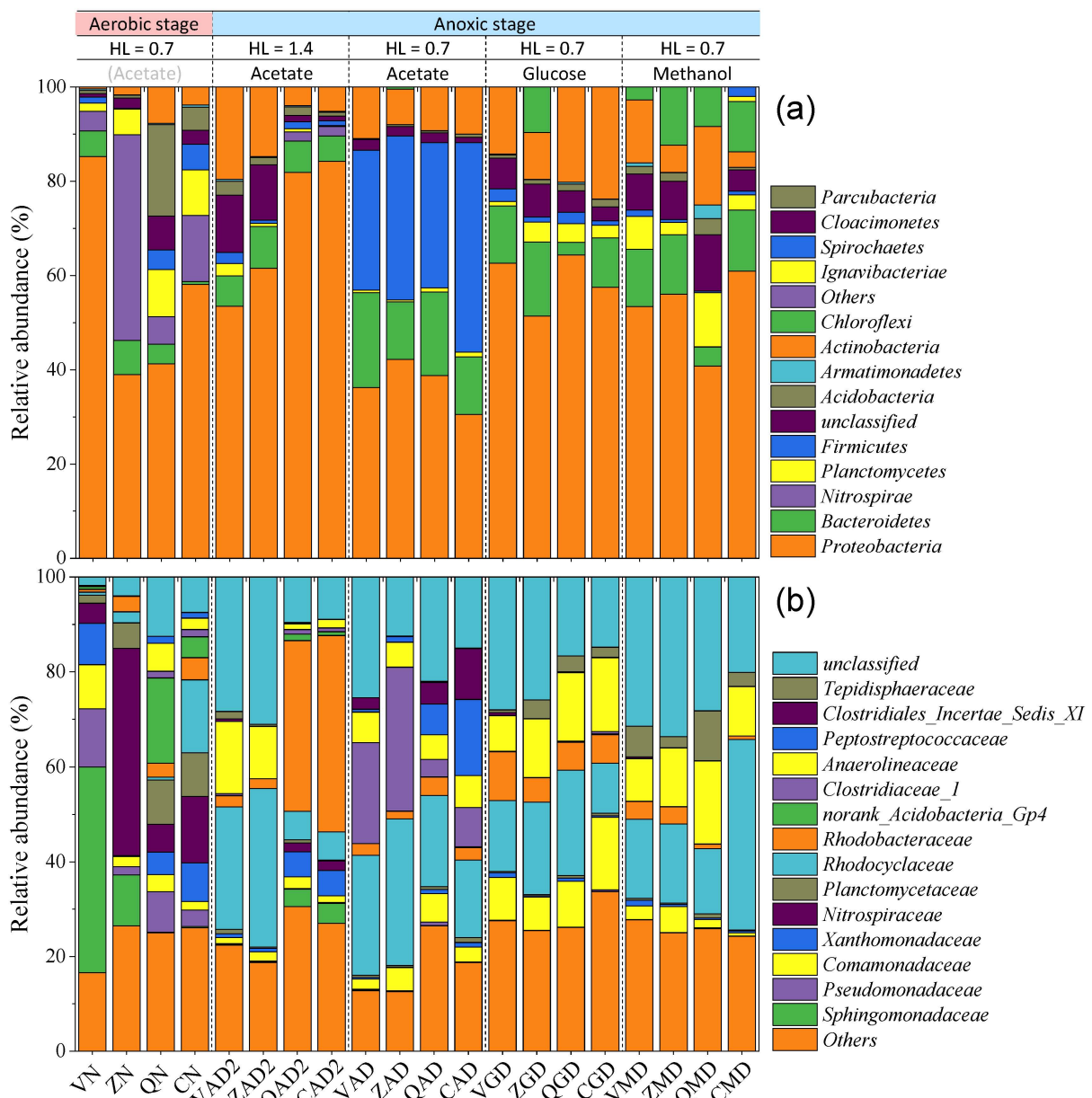


Figure 10. Relative abundance of microbial communities at (a) phylum and (b) family levels (<1% of the total sequences were reported as “others”).

To explore the distribution of the bacterial community in more detail, the genus level analysis is normally applied. However, because a large portion of sequences were not assigned clearly at the genus level (Figure S2), the family level analysis was deployed instead (Figure 10b). Coinciding with the results of phylum analysis, *Sphingomonadaceae*, *Pseudomonadaceae*, *Comamonadaceae*, *Xanthomonadaceae*, *Rhodocyclaceae*, and *Rhodobacteraceae* belonging to *Proteobacteria* are the dominant families. However, the abundances of *Clostridiaceae_1*, *Peptostreptococcaceae*, and *Clostridiales_Incertae_Sedis_XI* affiliating to *Firmicutes* were remarkable and varied significantly with the medium type for the samples (VAD, ZAD, QAD, and CAD). Meanwhile, the proportion of *Anaerolineaceae* of *Chloroflexi* were visibly less in the anoxic stages of the reactors fed by acetate as compared to those by glucose or methanol. Notably, at the genus level, *Sphingomonas*, an ammonia oxidizing bacteria (AOB) [48], and *Nitrospira*, a nitrite oxidizing bacteria (NOB), were extensively identified in VN and ZN, respectively (Figure S2). They were integrated with the abundant *Thauera* in the anoxic stage that plays important roles in low-carbon domestic sewage treatment [49],

ensuring efficient TN removal. In addition, the contents of *Clostridium_sensu_stricto* and *Proteiniclasticum* were higher when acetate was introduced into a volcanic- or zeolite-packed reactor (i.e., VAD and ZAD), where the former was the functional bacteria for hydrolysis and acidification and served as a denitrifier [50,51]. The overall taxonomic analysis indicates that the species of filter medium and carbon source significantly influenced the composition and/or diversity of the bacterial community.

4. Conclusions

In this work, the influences of the medium and carbon source on N removal from the simulated wastewater of the mining area of ionic rare earth using the biological aerated filter (BAF) was systematically investigated. Four mineral media including volcanic, zeolite, quartz, and ceramsite showed significant differences in terms of start-up performance and compatibility with soluble carbon sources (acetate, glucose, and methanol). Volcanic or quartz showed the more rapid start-up with respect to the other two, and compared with glucose and methanol, acetate was more compatible with the selected media as supported by the more favorable performance in N removal. For all medium-packed BAFs, a minimum C/N ratio of 3 was required to ensure the concentrations of TN and COD in the effluent were lower than the discharge standards, while which could be decreased by ~13% when solid sweet potato residue was introduced as the alternative electron donor. Blocking was first observed in the quartz-packed reactor followed by the zeolite, and ceramsite showed the best deblocking performance. The species of soluble carbon source significantly influenced the diversity of the bacterial community. For the samples collected from the anoxic stage when acetate was used, over 95% of the sequences were assigned to *Proteobacteria*, *Bacteroidetes*, *Firmicutes*, and *Actinobacteria*. Deploying volcanic as the medium and acetate as the soluble carbon source resulted in a simple ecosystem and is proposed for efficient N removal. Overall, the results obtained are important references for the engineering application of BAFs in coping with wastewater with low C/N ratio.

Supplementary Materials: The following supporting information can be downloaded at: <https://www.mdpi.com/article/10.3390/w14142246/s1>, Figure S1: Operational performance of (a) quartz- and (b) ceramsite-packed BAF after adding rice husk; Figure S2: Relative abundance of microbial community at genus level.

Author Contributions: Conceptualization, W.L.; Formal analysis, S.C.; Investigation, S.C. and C.W.; Methodology, S.C. and B.S.; Resources, M.C. and W.L.; Supervision, W.L.; Validation, S.C. and P.A.; Writing—original draft, S.C.; Writing—review and editing, W.L. All authors have read and agreed to the published version of the manuscript.

Funding: This research was funded by the National Key Research and Development Program of China (2019YFC1805100) and the Program of Qingjiang Excellent Young Talents, Jiangxi University of Science and Technology (JXUSTQJYX2020006).

Institutional Review Board Statement: Not applicable.

Informed Consent Statement: Not applicable.

Data Availability Statement: All data generated or analyzed during this study are included in this article.

Acknowledgments: The authors would like to thank Longwen Xiao and Hao Su for their help in the design and operation of the BAFs.

Conflicts of Interest: The authors declare no conflict of interest.

References

1. Galloway, J.N.; Townsend, A.R.; Erismann, J.W.; Bekunda, M.; Cai, Z.; Freney, J.R.; Martinelli, L.A.; Seitzinger, S.P.; Sutton, M.A. Transformation of the nitrogen cycle: Recent trends, questions, and potential solutions. *Science* **2008**, *320*, 889–892. [[CrossRef](#)] [[PubMed](#)]
2. Yin, S.; Chen, K.; Srinivasakannan, C.; Guo, S.; Li, S.; Peng, J.; Zhang, L. Enhancing recovery of ammonia from rare earth wastewater by air stripping combination of microwave heating and high gravity technology. *Chem. Eng. J.* **2018**, *337*, 515–521. [[CrossRef](#)]
3. Darestani, M.; Haigh, V.; Couperthwaite, S.J.; Millar, G.J.; Nghiem, L.D. Hollow fibre membrane contactors for ammonia recovery: Current status and future developments. *J. Environ. Chem. Eng.* **2017**, *5*, 1349–1359. [[CrossRef](#)]
4. Chen, Y.; Wang, N.; An, S.; Cai, C.; Peng, J.; Xie, M.; Peng, J.; Song, X. Synthesis of novel hierarchical porous zeolitization ceramsite from industrial waste as efficient adsorbent for separation of ammonia nitrogen. *Sep. Purif. Technol.* **2022**, *297*, 121418. [[CrossRef](#)]
5. Peng, Y.; Zhu, G. Biological nitrogen removal with nitrification and denitrification via nitrite pathway. *Appl. Microbiol. Biotechnol.* **2006**, *73*, 15–26. [[CrossRef](#)]
6. Carrera, J.; Baeza, J.A.; Vicent, T.; Lafuente, J. Biological nitrogen removal of high-strength ammonium industrial wastewater with two-sludge system. *Water Res.* **2003**, *37*, 4211–4221. [[CrossRef](#)]
7. Pujol, R.; Hamon, M.; Kandel, X.; Lemmel, H. Biofilters: Flexible, reliable biological reactors. *Water Sci. Technol.* **1994**, *29*, 33–38. [[CrossRef](#)]
8. Gonçalves, R.F.; Araújo, V.L.d.; Chernicharo, C.A.L. Association of a UASB reactor and a submerged aerated biofilter for domestic sewage treatment. *Water Sci. Technol.* **1998**, *38*, 189–195. [[CrossRef](#)]
9. Rahimi, Y.; Torabian, A.; Mehrdadi, N.; Shahmoradi, B. Simultaneous nitrification-denitrification and phosphorus removal in a fixed bed sequencing batch reactor (FBSBR). *J. Hazard. Mater.* **2011**, *185*, 852–857. [[CrossRef](#)]
10. Müller, N. Implementing biofilm carriers into activated sludge process—15 years of experience. *Water Sci. Technol.* **1998**, *37*, 167–174. [[CrossRef](#)]
11. Ji, G.; Tong, J.; Tan, Y. Wastewater treatment efficiency of a multi-media biological aerated filter (MBAF) containing clinoptilolite and bioceramsite in a brick-wall embedded design. *Bioresour. Technol.* **2011**, *102*, 550–557. [[CrossRef](#)] [[PubMed](#)]
12. Huang, X.; Wang, Y.; Wang, W.; Li, B.; Zhao, K.; Kou, X.; Wu, S.; Shao, T. Simultaneous partial nitritation, anammox, and denitrification process for the treatment of simulated municipal sewage in a single-stage biofilter reactor. *Chemosphere* **2022**, *287*, 131974. [[CrossRef](#)] [[PubMed](#)]
13. Yang, B.; Wang, J.; Wang, J.; Xu, H.; Song, X.; Wang, Y.; Li, F.; Liu, Y.; Bai, J. Correlating microbial community structure with operational conditions in biological aerated filter reactor for efficient nitrogen removal of municipal wastewater. *Bioresour. Technol.* **2018**, *250*, 374–381. [[CrossRef](#)]
14. An, Y.; Li, S.; Wang, X.; Liu, Y.; Wang, R. Correlating Microbial Community Characteristics with Environmental Factors along a Two-Stage Biological Aerated Filter. *Water* **2020**, *12*, 3317. [[CrossRef](#)]
15. Chen, Z.; Wang, X.; Chen, X.; Yang, Y.; Gu, X. Pilot study of nitrogen removal from landfill leachate by stable nitritation-denitrification based on zeolite biological aerated filter. *Waste Manag.* **2019**, *100*, 161–170. [[CrossRef](#)] [[PubMed](#)]
16. Nie, W.; Zhang, R.; He, Z.; Zhou, J.; Wu, M.; Xu, Z.; Chi, R.; Yang, H. Research progress on leaching technology and theory of weathered crust elution-deposited rare earth ore. *Hydrometallurgy* **2020**, *193*, 105295. [[CrossRef](#)]
17. Mendoza-Espinosa, L.; Stephenson, T. A review of biological aerated filters (BAFs) for wastewater treatment. *Environ. Eng. Sci.* **1999**, *16*, 201–216. [[CrossRef](#)]
18. Dong, Y.; Lin, H.; Zhang, X. Simultaneous ammonia nitrogen and phosphorus removal from micro-polluted water by biological aerated filters with different media. *Water Air Soil Pollut.* **2020**, *231*, 234. [[CrossRef](#)]
19. Feng, Y.; Yu, Y.; Duan, Q.; Tan, J.; Zhao, C. The characteristic research of ammonium removal in grain-slag biological aerated filter (BAF). *Desalination* **2010**, *263*, 146–150. [[CrossRef](#)]
20. Qiu, L.; Zhang, S.; Wang, G.; Du, M.a. Performances and nitrification properties of biological aerated filters with zeolite, ceramic particle and carbonate media. *Bioresour. Technol.* **2010**, *101*, 7245–7251. [[CrossRef](#)]
21. Constantin, H.; Fick, M. Influence of C-sources on the denitrification rate of a high-nitrate concentrated industrial wastewater. *Water Res.* **1997**, *31*, 583–589. [[CrossRef](#)]
22. Xu, Z.; Dai, X.; Chai, X. Effect of different carbon sources on denitrification performance, microbial community structure and denitrification genes. *Sci. Total Environ.* **2018**, *634*, 195–204. [[CrossRef](#)] [[PubMed](#)]
23. Her, J.-J.; Huang, J.-S. Influences of carbon source and C/N ratio on nitrate/nitrite denitrification and carbon breakthrough. *Bioresour. Technol.* **1995**, *54*, 45–51. [[CrossRef](#)]
24. Liang, X.; Lin, L.; Ye, Y.; Gu, J.; Wang, Z.; Xu, L.; Jin, Y.; Ru, Q.; Tian, G. Nutrient removal efficiency in a rice-straw denitrifying bioreactor. *Bioresour. Technol.* **2015**, *198*, 746–754. [[CrossRef](#)]
25. Chang, J.; Ma, L.; Zhou, Y.; Zhang, S.; Wang, W. Remediation of nitrate-contaminated wastewater using denitrification biofilters with straws of ornamental flowers added as carbon source. *Water Sci. Technol.* **2016**, *74*, 416–423. [[CrossRef](#)]
26. Schipper, L.A.; Robertson, W.D.; Gold, A.J.; Jaynes, D.B.; Cameron, S.C. Denitrifying bioreactors—An approach for reducing nitrate loads to receiving waters. *Ecol. Eng.* **2010**, *36*, 1532–1543. [[CrossRef](#)]
27. Jiang, Y.; Li, Y.; Zhang, Y.; Zhang, X. Effects of HRT on the efficiency of denitrification and carbon source release in constructed wetland filled with bark. *Water Sci. Technol.* **2017**, *75*, 2908–2915. [[CrossRef](#)] [[PubMed](#)]

28. Makarem, M.; Lee, C.M.; Kafle, K.; Huang, S.; Chae, I.; Yang, H.; Kubicki, J.D.; Kim, S.H. Probing cellulose structures with vibrational spectroscopy. *Cellulose* **2019**, *26*, 35–79. [[CrossRef](#)]
29. Jiang, L.; Zhang, Y.; Shen, Q.; Mao, Y.; Zhang, Q.; Ji, F. The metabolic patterns of the complete nitrates removal in the biofilm denitrification systems supported by polymer and water-soluble carbon sources as the electron donors. *Bioresour. Technol.* **2021**, *342*, 126002. [[CrossRef](#)]
30. Henze, M. Capabilities of biological nitrogen removal processes from wastewater. *Water Sci. Technol.* **1991**, *23*, 669–679. [[CrossRef](#)]
31. Liu, M.; Zhou, S.; Li, Y.; Tian, J.; Zhang, C. Structure, physicochemical properties and effects on nutrients digestion of modified soluble dietary fiber extracted from sweet potato residue. *Food Res. Int.* **2021**, *150*, 110761. [[CrossRef](#)] [[PubMed](#)]
32. Feng, Y.; Qi, J.; Chi, L.; Wang, D.; Wang, Z.; Li, K.; Li, X. Production of sorption functional media (SFM) from clinoptilolite tailings and its performance investigation in a biological aerated filter (BAF) reactor. *J. Hazard. Mater.* **2013**, *246–247*, 61–69. [[CrossRef](#)] [[PubMed](#)]
33. Bao, T.; Chen, T.; Wille, M.-L.; Chen, D.; Bian, J.; Qing, C.; Wu, W.; Frost, R.L. Advanced wastewater treatment with autoclaved aerated concrete particles in biological aerated filters. *J. Water Process Eng.* **2016**, *9*, 188–194. [[CrossRef](#)]
34. Wen, D.; Ho, Y.S.; Tang, X. Comparative sorption kinetic studies of ammonium onto zeolite. *J. Hazard. Mater.* **2006**, *133*, 252–256. [[CrossRef](#)] [[PubMed](#)]
35. Yue, X.; Yu, G.; Liu, Z.; Tang, J.; Liu, J. Fast start-up of the CANON process with a SABF and the effects of pH and temperature on nitrogen removal and microbial activity. *Bioresour. Technol.* **2018**, *254*, 157–165. [[CrossRef](#)]
36. Wang, S.; Zhou, M.; Zeng, L.; Dai, W. Investigation on the preparation and properties of reticulate porous ceramic for organism carrier in sewage disposal. *J. Ceramic Process. Res.* **2016**, *17*, 1095–1099.
37. Galvez, A.; Zamorano, M.; Ramos-Ridao, A.F. Efficiency of a biological aerated filter for the treatment of leachate produced at a landfill receiving non-recyclable waste. *J. Environ. Sci. Health A* **2012**, *47*, 54–59. [[CrossRef](#)]
38. Yue, X.; Yu, G.; Lu, Y.; Liu, Z.; Li, Q.; Tang, J.; Liu, J. Effect of dissolved oxygen on nitrogen removal and the microbial community of the completely autotrophic nitrogen removal over nitrite process in a submerged aerated biological filter. *Bioresour. Technol.* **2018**, *254*, 67–74. [[CrossRef](#)]
39. Elefsiniotis, P.; Wareham, D.G.; Smith, M.O. Use of volatile fatty acids from an acid-phase digester for denitrification. *J. Biotechnol.* **2004**, *114*, 289–297. [[CrossRef](#)]
40. Fu, X.; Hou, R.; Yang, P.; Qian, S.; Feng, Z.; Chen, Z.; Wang, F.; Yuan, R.; Chen, H.; Zhou, B. Application of external carbon source in heterotrophic denitrification of domestic sewage: A review. *Sci. Total Environ.* **2022**, *817*, 153061. [[CrossRef](#)]
41. Volokita, M.; Abeliovich, A.; Soares, M.I.M. Denitrification of groundwater using cotton as energy source. *Water Sci. Technol.* **1996**, *34*, 379–385. [[CrossRef](#)]
42. Shao, L.; Xu, Z.; Jin, W.; Yin, H. Rice husk as carbon source and biofilm carrier for water denitrification. *Pol. J. Environ. Stud.* **2009**, *18*, 693–699. [[CrossRef](#)]
43. Luo, Z.; Li, S.; Zhu, X.; Ji, G. Carbon source effects on nitrogen transformation processes and the quantitative molecular mechanism in long-term flooded constructed wetlands. *Ecol. Eng.* **2018**, *123*, 19–29. [[CrossRef](#)]
44. Cameron, S.G.; Schipper, L.A. Nitrate removal and hydraulic performance of organic carbon for use in denitrification beds. *Ecol. Eng.* **2010**, *36*, 1588–1595. [[CrossRef](#)]
45. Jiang, F.; Qi, Y.; Shi, X. Effect of liquid carbon sources on nitrate removal, characteristics of soluble microbial products and microbial community in denitrification biofilters. *J. Clean. Prod.* **2022**, *339*, 130776. [[CrossRef](#)]
46. Li, Y.; Guo, J.; Li, H.; Song, Y.; Chen, Z.; Lu, C.; Han, Y.; Hou, Y. Effect of dissolved oxygen on simultaneous removal of ammonia, nitrate and phosphorus via biological aerated filter with sulfur and pyrite as composite fillers. *Bioresour. Technol.* **2020**, *296*, 122340. [[CrossRef](#)]
47. Jones, R.T.; Robeson, M.S.; Lauber, C.L.; Hamady, M.; Knight, R.; Fierer, N. A comprehensive survey of soil acidobacterial diversity using pyrosequencing and clone library analyses. *ISME J.* **2009**, *3*, 442–453. [[CrossRef](#)]
48. Antwi, P.; Zhang, D.; Su, H.; Luo, W.; Quashie, F.K.; Kabutey, F.T.; Xiao, L.; Lai, C.; Liu, Z.; Li, J. Nitrogen removal from landfill leachate by single-stage anammox and partial-nitritation process: Effects of microaerobic condition on performance and microbial activities. *J. Water Process. Eng.* **2020**, *38*, 101572. [[CrossRef](#)]
49. Ren, T.; Chi, Y.; Wang, Y.; Shi, X.; Jin, X.; Jin, P. Diversified metabolism makes novel *Thauera* strain highly competitive in low carbon wastewater treatment. *Water Res.* **2021**, *206*, 117742. [[CrossRef](#)]
50. Zheng, Y.; Sun, Z.; Liu, Y.; Cao, T.; Zhang, H.; Hao, M.; Chen, R.; Dzakpasu, M.; Wang, X.C. Phytoremediation mechanisms and plant eco-physiological response to microorganic contaminants in integrated vertical-flow constructed wetlands. *J. Hazard. Mater.* **2022**, *424*, 127611. [[CrossRef](#)]
51. Liu, J.; Liu, X.; Gao, L.; Xu, S.; Chen, X.; Tian, H.; Kang, X. Performance and microbial community of a novel combined anaerobic bioreactor integrating anaerobic baffling and anaerobic filtration process for low-strength rural wastewater treatment. *Environ. Sci. Pollut. Res.* **2020**, *27*, 18743–18756. [[CrossRef](#)] [[PubMed](#)]